

# Multi-Antenna SWIPT Systems With Joint Time Switching

Hoon Lee, <sup>†</sup>Kyoung-Jae Lee, Hanjin Kim, and Inkyu Lee, *Fellow, IEEE*  
School of Electrical Eng., Korea University, Seoul, Korea

<sup>†</sup>Dep. of Electronics and Control Eng., Hanbat National University, Daejeon, Korea  
Email: {ihun1, hanjin8612, inkyu}@korea.ac.kr, <sup>†</sup>kyoungjae@hanbat.ac.kr

**Abstract**—In this paper, we investigate simultaneous wireless information and power transfer (SWIPT) where a multi-antenna transmitter sends data and energy to single antenna receivers with a time switching (TS) circuit. In this system, a general joint TS protocol is introduced which includes conventional TS schemes as special cases. We aim to analyze the achievable rate region of the joint TS under energy harvesting constraint at the receivers by jointly optimizing the TS ratios and the transmit covariance matrices. To tackle non-convex rate region characterization problems, we first decouple the original problems into several subproblems with fixed auxiliary variables. Then, the globally optimal TS ratios and the transmit covariance matrices are computed via convex optimization techniques. Numerical examples verify the efficacy of the proposed joint TS over conventional methods.

## I. INTRODUCTION

In recent years, simultaneous wireless information and power transfer (SWIPT) has been intensively studied in many literature [1]–[7] owing to its capability of supplying power and transmitting data to mobile devices at the same time. The authors in [1] first applied multi-antenna techniques to the SWIPT. To support concurrent information decoding (ID) and energy harvesting (EH) operations at a receiver, [1] proposed power splitting (PS) and time switching (TS) architectures for point-to-point systems. In specific, the PS receiver splits the received signal at each antenna into ID and EH parts, while the TS circuit dynamically switches the role of a receiver between the ID and the EH modes. These results for the PS and the TS methods have been extended to multi-user networks [8]–[16].

Although a much simpler circuit structure is possible for the TS receiver, most works on the downlink multi-user SWIPT focused on the PS receiver structure [8]–[10]. When we design the TS-based SWIPT protocols in the multi-user systems, a main challenge is how to handle asynchronous modes of multiple users caused by different TS ratio settings at users. Also, in the TS methods, the users can dynamically change their modes in order to improve the system performance. Furthermore, since the optimal beamforming depends on the modes of users [1] [4], a transmission strategy should be carefully optimized according to the users' ID and EH modes.

Several recent works studied the TS-based SWIPT systems [13] [14]. Time division based TS techniques were introduced for the SWIPT MISO interference channels in [12]. However, the transmitters are assumed to apply the same beamforming vectors regardless of the receivers' modes. Moreover, the asynchronous ID and EH modes among multiple users were not considered in [12] due to time division concepts.

This work was supported by the National Research Foundation through the Ministry of Science, ICT, and Future Planning (MSIP), Korean Government under Grant 2017R1A2B3012316. The work of K.-J. Lee was supported by Korea Evaluation Institute of Industrial Technology (KEIT) grant funded by the Korea government (MOTIE) (No.10079984, Development of non-binding multimodal wireless power transfer technology for wearable device).

The TS methods were extended to multi-cell multi-user MISO networks [13] [14]. In [13], a transmit TS scheme was proposed, and the minimum rate maximization and the transmit power minimization problems were solved based on the path-following algorithms. Compared to [12], the performance of the SWIPT system in [13] was fairly improved by separately designing the beamforming vectors for the EH and the ID time durations. However, [13] assumed that all the users employ the same TS ratio for the EH mode.

Such an issue would be resolved by adopting a receive TS method presented in [14], where the EH durations of different users are not the same, i.e., the users can employ different TS ratios based on their energy or information rate constraint. For multi-cell MISO systems, multi-objective optimization problems were addressed in [14] where both the information rate and the harvested energy were simultaneously maximized. Nevertheless, the performance of the TS-based SWIPT cannot be fully evaluated in [14], since the same transmit beamforming strategy is applied for the information and the energy transmission.

In this paper, we present a new joint TS protocol for a two-user MISO broadcast channel (BC) which include the conventional TS-based SWIPT methods in [13] and [14] as special cases. In the joint TS scheme, depending on the modes of the receivers, there exist four individual cases which have three different phases. Then, transmit covariance matrices are dynamically optimized for all different phases, and the TS ratio is jointly determined with the transmitter optimization.

We identify the achievable rate region of the proposed joint TS under EH constraint at each user as well as average power and peak power constraint at a transmitter. To optimally solve non-convex problems, we first decouple the original problems into three different subproblems and derive the optimal transmit covariance matrices with given TS ratios. Then, based on the convexity proof of the average power minimization problems, the optimal TS ratios can be efficiently obtained by the subgradient methods. Numerical examples verify that the proposed joint TS method generates much larger rate region compared to the conventional TS-based SWIPT schemes.

## II. SYSTEM MODEL

As shown in Fig. 1, we consider a two-user MISO SWIPT BC where each receiver with a single antenna decodes information and harvests energy by using the signals from a transmitter equipped with  $M$  antennas. For the SWIPT, we apply the TS circuit at the receivers so that they can change their modes between an ID mode and an EH mode. Without loss of generality, the total transmission time is assumed to be one, and the time durations of receiver  $i$  ( $i = 1, 2$ ) for the ID and the EH modes are equal to  $\tau_i$  and  $1 - \tau_i$ , respectively.

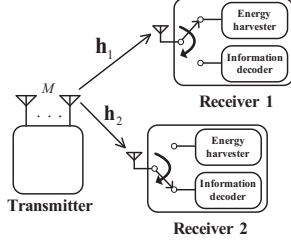


Fig. 1. Schematic diagram for a two-user MISO BC with TS receivers

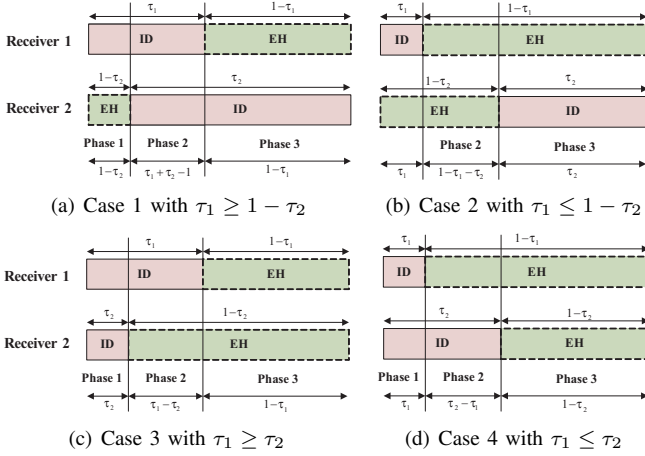


Fig. 2. Four cases for the frame structure in the joint TS protocol

In this system, according to the modes of the receivers, there exist four different frame structures as illustrated in Fig. 2. Note that cases 1 and 2, which are respectively shown in Fig. 2 (a) and (b), indicate scenarios where the order of the ID and the EH modes is reversed for each user. In contrast, for cases 3 and 4 in Fig. 2 (c) and (d), respectively, both receivers first decode information and then change their operations to the EH mode. In all cases, the total system block is divided into three phases each of which has different duration depending on the relation between  $\tau_1$  and  $\tau_2$ . In phase  $j$  ( $j = 1, 2, 3$ ), the transmitter employs a transmit covariance matrix  $\mathbf{Q}_{ij} \in \mathbb{C}^{M \times M}$  for receiver  $i$  to transfer data or energy. Then, in each case, six transmit covariance matrices  $\{\mathbf{Q}_{ij}\}$  and two TS ratios  $\{\tau_i\}$  should be optimized.

In order to jointly design  $\{\mathbf{Q}_{ij}\}$  and  $\{\tau_i\}$ , the transmitter and the receivers cooperatively switch their information and energy transmission/reception modes. Thus, a protocol in Fig. 2 is named as a joint TS scheme. Note that the proposed joint TS includes both the transmit TS [13] and the receive TS [14] as special cases, which will be clarified in Section II-C. In this paper, we identify the achievable rate region of the proposed joint TS scheme under EH constraint at the receivers. In the following subsections, we first describe a system model, and then it is followed by the problem formulation.

#### A. Case 1

In case 1 (Fig. 2 (a)), the ID operations of the receivers are overlapped for  $\tau_1 + \tau_2 - 1 \geq 0$  duration. Let us denote  $\mathbf{h}_i \in \mathbb{C}^{M \times 1}$  as the quasi-static flat-fading channel vector from the transmitter to receiver  $i$  which is assumed to be constant for one transmission block. Then, the received signal  $y_{ij}$  at receiver  $i$  in phase  $j$  is expressed as  $y_{ij} = \mathbf{h}_i^H (\mathbf{x}_{1j} + \mathbf{x}_{2j}) + z_{ij}$ ,

where  $\mathbf{x}_{ij} \sim \mathcal{CN}(\mathbf{0}, \mathbf{Q}_{ij})$  stands for the transmitted signal for receiver  $i$  in phase  $j$ , and  $z_{ij} \sim \mathcal{CN}(0, 1)$  indicates the complex Gaussian noise at receiver  $i$  in phase  $j$ .

In phase 1 of duration  $1 - \tau_2$ , receiver 1 decodes information while receiver 2 harvests energy of the received signal. Thus, the transmit covariance matrix  $\mathbf{Q}_{21}$  for receiver 2 becomes  $\mathbf{Q}_{21} = \mathbf{0}$ , since the dedicated energy beamforming is not required for the SWIPT [1] [2]. Then, the achievable rate at receiver 1 and the harvested energy at receiver 2 can be respectively written by [1]

$$\begin{aligned} R_{11}^{(1)} &= (1 - \tau_2) \log(1 + \mathbf{h}_1^H \mathbf{Q}_{11} \mathbf{h}_1), \\ E_{21}^{(1)} &= \eta_2 (1 - \tau_2) \mathbf{h}_2^H \mathbf{Q}_{11} \mathbf{h}_2, \end{aligned}$$

where  $R_{ij}^{(n)}$  and  $E_{ij}^{(n)}$  represent the achievable rate and the harvested energy at receiver  $i$  in phase  $j$  for case  $n$  ( $n = 1, \dots, 4$ ), respectively, and  $\eta_i \in (0, 1]$  reflects the EH efficiency at receiver  $i$ . Unless stated otherwise, we set  $\eta_1 = \eta_2 = 1$  for notational simplicity.

Next, in phase 2 with duration  $\tau_1 + \tau_2 - 1$ , both receivers operate in the ID mode, and the achievable rate  $R_{i2}^{(1)}$  of receiver  $i$  is given by

$$R_{i2}^{(1)} = (\tau_1 + \tau_2 - 1) \log \left( 1 + \frac{\mathbf{h}_i^H \mathbf{Q}_{i2} \mathbf{h}_i}{1 + \mathbf{h}_i^H \mathbf{Q}_{i2} \mathbf{h}_i} \right),$$

where we define  $\bar{i} = 1$  for  $i = 2$  and  $\bar{i} = 2$  for  $i = 1$ . Finally, for the remaining duration  $1 - \tau_1$ , receiver 1 collects energy from the received signal, whereas receiver 2 becomes an ID receiver. Accordingly, in phase 3, the harvested energy  $E_{13}^{(1)}$  and the rate  $R_{23}^{(1)}$  are respectively derived as

$$\begin{aligned} E_{13}^{(1)} &= (1 - \tau_1) \mathbf{h}_1^H \mathbf{Q}_{23} \mathbf{h}_1, \\ R_{23}^{(1)} &= (1 - \tau_1) \log(1 + \mathbf{h}_2^H \mathbf{Q}_{23} \mathbf{h}_2), \end{aligned}$$

where the energy transmit covariance matrix  $\mathbf{Q}_{13}$  is set to  $\mathbf{Q}_{13} = \mathbf{0}$  as in phase 1. Hence, the total achievable rate for each receiver can be attained as  $R_1^{(1)} = R_{11}^{(1)} + R_{12}^{(1)}$  and  $R_2^{(1)} = R_{22}^{(1)} + R_{23}^{(1)}$ , where  $R_i^{(n)}$  reflects the total achievable rate at receiver  $i$  for case  $n$ .

Let us denote  $P_A$  and  $P_P$  as the average power and the peak power budget at the transmitter, respectively. Then, the transmit covariance matrices  $\{\mathbf{Q}_{ij}\}$  and the TS ratios  $\{\tau_i\}$  should satisfy the following power constraints:

$$\begin{aligned} (1 - \tau_2) \text{tr}(\mathbf{Q}_{11}) + (\tau_1 + \tau_2 - 1) \text{tr}(\mathbf{Q}_{12} + \mathbf{Q}_{22}) \\ + (1 - \tau_1) \text{tr}(\mathbf{Q}_{23}) \leq P_A, \quad (1) \\ \text{tr}(\mathbf{Q}_{11}) \leq P_P, \text{tr}(\mathbf{Q}_{12} + \mathbf{Q}_{22}) \leq P_P, \text{tr}(\mathbf{Q}_{23}) \leq P_P. \quad (2) \end{aligned}$$

Also, in order to fulfill the minimum required EH constraint  $e_i$  for receiver  $i$ , we have

$$\begin{aligned} E_1^{(1)} &= E_{13}^{(1)} = (1 - \tau_1) \mathbf{h}_1^H \mathbf{Q}_{23} \mathbf{h}_1 \geq e_1, \quad (3) \\ E_2^{(1)} &= E_{21}^{(1)} = (1 - \tau_2) \mathbf{h}_2^H \mathbf{Q}_{11} \mathbf{h}_2 \geq e_2, \quad (4) \end{aligned}$$

where  $E_i^{(n)}$  equals the total harvested energy at receiver  $i$  for case  $n$ . In addition, the feasible set for  $\tau_1$  and  $\tau_2$  in case 1 can be represented as

$$\tau_1 + \tau_2 \geq 1 \quad (5)$$

since the durations for the ID modes of two receivers are overlapped in case 1 (see Fig. 2 (a)). With given  $\{e_i\}$ ,  $P_A$ ,

and  $P_P$ , the feasible set  $\mathcal{F}^{(1)}$  of  $\{\mathbf{Q}_{ij}\}$  and  $\{\tau_i\}$  for case 1 can be specified by (1)-(5).

The system models for the remaining cases are similar to case 1. For the details, please refer to the journal version of this paper [17].

### B. Problem Formulation

In this subsection, we formulate problems for determining the boundary points of the achievable rate region  $\mathcal{R}$  of the proposed joint TS scheme. The region  $\mathcal{R}$  can be represented as  $\mathcal{R} = \bigcup_{n=1}^4 \mathcal{R}^{(n)}$ , where the set  $\mathcal{R}^{(n)}$  indicates the rate region for case  $n$  which is denoted by

$$\mathcal{R}^{(n)} = \bigcup_{(\{\tau_i\}, \{\mathbf{Q}_{ij}\}) \in \mathcal{F}^{(n)}} \{(r_1, r_2) : r_i \leq R_i^{(n)}, 0 \leq \tau_i \leq 1, \mathbf{Q}_{ij} \succeq \mathbf{0}, \forall i, j\}.$$

with  $\mathcal{F}^{(n)}$  equal to the feasible set of  $\{\mathbf{Q}_{ij}\}$  and  $\{\tau_i\}$  for case  $n$ . In order to fully characterize the boundary points of  $\mathcal{R}^{(n)}$  for  $n = 1, \dots, 4$ , we adopt the rate profile approach [18] which maximizes the sum rate  $r_{sum} = R_1^{(n)} + R_2^{(n)}$  such that the ratio between  $r_{sum}$  and  $R_i^{(n)}$  is given by  $\frac{R_1^{(n)}}{r_{sum}} = \alpha$  and  $\frac{R_2^{(n)}}{r_{sum}} = 1 - \alpha$  with a predefined profile parameter  $\alpha \in [0, 1]$ . For case  $n$ , the sum rate maximization problem with a fixed  $\alpha$  is then formulated as

$$\begin{aligned} \text{(P)} : \quad & \max_{\{0 \leq \tau_i \leq 1\}, \{\mathbf{Q}_{ij} \succeq \mathbf{0}\}, r_{sum} \geq 0} r_{sum} \\ & \text{s.t. } R_1^{(n)} \geq \alpha r_{sum}, R_2^{(n)} \geq (1 - \alpha) r_{sum}, \quad (6) \\ & (\{\tau_i\}, \{\mathbf{Q}_{ij}\}) \in \mathcal{F}^{(n)}. \end{aligned}$$

It is well known that by solving (P) for all possible  $\alpha$ , we can efficiently obtain the boundary points of  $\mathcal{R}^{(n)}$  [18]. However, (P) is non-convex in general due to the coupled variables and the non-convex constraint functions.

### C. Conventional TS-based SWIPT Schemes

Before solving (P), we briefly review two conventional TS schemes [13] [14], and verify that both the conventional methods are special cases of the proposed joint TS.

1) *Transmit TS* [13]: The transmit TS scheme adopts the frame structure of case 3 or 4 with  $\tau_1 = \tau_2$ , and different covariance matrices are utilized for information and energy transmission. Then, the achievable rate region of the transmit TS  $\mathcal{R}_{\text{Tx}}$  can be interpreted as  $\mathcal{R}_{\text{Tx}} \subseteq \mathcal{R}^{(3)} \cap \mathcal{R}^{(4)}$ .

2) *Receive TS* [14]: In the receive TS, the receivers opportunisticly choose their ID mode durations  $\{\tau_i\}$ , but the transmitter employs the same covariance matrix during all three phases  $\mathbf{Q}_{i1} = \mathbf{Q}_{i2} = \mathbf{Q}_{i3}, \forall i$ . Thus, the receive TS is given by a subset of case 3 and 4, i.e.,  $\mathcal{R}_{\text{Rx}} \subseteq \mathcal{R}^{(3)} \cup \mathcal{R}^{(4)}$ , where  $\mathcal{R}_{\text{Rx}}$  indicates the rate region of the receive TS.

## III. OPTIMAL SOLUTION

In this section, we investigate the optimal solution for the sum rate maximization problem (P) for case 1. To this end, with a given  $r_{sum}$ , we first consider the following average power minimization problem at the transmitter under the EH and peak power constraint.

$$\begin{aligned} & \min_{\{0 \leq \tau_i \leq 1\}, \{\mathbf{Q}_{ij} \succeq \mathbf{0}\}} (1 - \tau_2) \text{tr}(\mathbf{Q}_{11}) \\ & \quad + (\tau_1 + \tau_2 - 1) \text{tr}(\mathbf{Q}_{12} + \mathbf{Q}_{22}) + (1 - \tau_1) \text{tr}(\mathbf{Q}_{23}) \quad (7) \\ & \text{s.t. } R_1^{(1)} \geq \alpha r_{sum}, R_2^{(1)} \geq (1 - \alpha) r_{sum}. \end{aligned}$$

Let us denote  $p_A^*$  as the optimal value of (7), which reflects the minimum average transmit power required to achieve a given sum rate  $r_{sum}$ . Then, we can check that  $r_{sum}$  is a feasible solution for (P) when  $p_A^* \leq P_A$ . Otherwise, the sum rate  $r_{sum}$  is not achievable with a given average power budget  $P_A$ , and thus it is infeasible for (P). Hence, one can identify the optimal sum rate  $r_{sum}^*$  by the bisection method in an outer layer, whose optimality and convergence have been proved in [18].

Thus, we focus on an inner layer procedure that solves the average power minimization problem (7), which is still non-convex in general. To tackle the non-convexity, we decouple the original problem (7) into several subproblems, which will be verified as convex optimization problems. Then, the boundary of the achievable rate region can be optimally calculated by solving those convex subproblems instead of examining the non-convex one in (7).

Let us introduce auxiliary variables  $\{r_{ij} \geq 0\}$ , which represent the achievable rate of receiver  $i$  in phase  $j$ , as

$$(1 - \tau_2) \log(1 + \mathbf{h}_1^H \mathbf{Q}_{11} \mathbf{h}_1) \geq r_{11}, \quad (8)$$

$$(\tau_1 + \tau_2 - 1) \log\left(1 + \frac{\mathbf{h}_1^H \mathbf{Q}_{12} \mathbf{h}_1}{1 + \mathbf{h}_1^H \mathbf{Q}_{22} \mathbf{h}_1}\right) \geq r_{12}, \quad (9)$$

$$(\tau_1 + \tau_2 - 1) \log\left(1 + \frac{\mathbf{h}_2^H \mathbf{Q}_{22} \mathbf{h}_2}{1 + \mathbf{h}_2^H \mathbf{Q}_{12} \mathbf{h}_2}\right) \geq r_{22}, \quad (10)$$

$$(1 - \tau_1) \log(1 + \mathbf{h}_2^H \mathbf{Q}_{23} \mathbf{h}_2) \geq r_{23}. \quad (11)$$

Also, defining new optimization variables  $\{\mathbf{W}_{ij}\}$  as

$$\begin{aligned} \mathbf{W}_{11} &= (1 - \tau_2) \mathbf{Q}_{11}, \quad \mathbf{W}_{i2} = (\tau_1 + \tau_2 - 1) \mathbf{Q}_{i2}, \quad i = 1, 2, \\ & \text{and } \mathbf{W}_{23} = (1 - \tau_1) \mathbf{Q}_{23}, \quad (12) \end{aligned}$$

we have the following theorem which addresses an equivalent problem of (7).

*Theorem 1:* The minimum required average power  $p_A^*$  in (7) can be equivalently computed as (P1) on the top of the next page, where  $\gamma_{11}(\tau_2, r_{11}) \triangleq f(1 - \tau_2, r_{11})$ ,  $\gamma_{k2}(\{\tau_i\}, r_{k2}) \triangleq f(\tau_1 + \tau_2 - 1, r_{k2})$ ,  $k = 1, 2$ , and  $\gamma_{23}(\tau_1, r_{23}) \triangleq f(1 - \tau_1, r_{23})$  with  $f(t, x) \triangleq t(\exp(\frac{x}{t}) - 1)$ . Here, the functions  $\{p_j^*(\cdot)\}$  can be obtained as

$$\begin{aligned} \text{(P1.1)} : \quad & p_1^*(\tau_2, r_{11}) \triangleq \min_{\mathbf{W}_{11} \succeq \mathbf{0}} \text{tr}(\mathbf{W}_{11}) \\ & \text{s.t. } \mathbf{h}_1^H \mathbf{W}_{11} \mathbf{h}_1 \geq \gamma_{11}(\tau_2, r_{11}), \quad (17) \\ & \mathbf{h}_2^H \mathbf{W}_{11} \mathbf{h}_2 \geq e_2, \quad (18) \\ & \text{tr}(\mathbf{W}_{11}) \leq P_P(1 - \tau_2), \quad (19) \end{aligned}$$

$$\begin{aligned} \text{(P1.2)} : \quad & p_2^*(\{\tau_i\}, \{r_{i2}\}) \\ & \triangleq \min_{\{\mathbf{W}_{i2} \succeq \mathbf{0}\}} \text{tr}(\mathbf{W}_{12} + \mathbf{W}_{22}) \\ & \text{s.t. } \mathbf{h}_1^H \mathbf{W}_{12} \mathbf{h}_1 - \frac{\gamma_{12}(\{\tau_i\}, r_{12})}{\tau_1 + \tau_2 - 1} \mathbf{h}_1^H \mathbf{W}_{22} \mathbf{h}_1 \geq \gamma_{12}(\{\tau_i\}, r_{12}), \quad (20) \\ & \mathbf{h}_2^H \mathbf{W}_{22} \mathbf{h}_2 - \frac{\gamma_{22}(\{\tau_i\}, r_{22})}{\tau_1 + \tau_2 - 1} \mathbf{h}_2^H \mathbf{W}_{12} \mathbf{h}_2 \geq \gamma_{22}(\{\tau_i\}, r_{22}), \quad (21) \\ & \text{tr}(\mathbf{W}_{12} + \mathbf{W}_{22}) \leq P_P(\tau_1 + \tau_2 - 1), \quad (22) \end{aligned}$$

$$\begin{aligned} \text{(P1.3)} : \quad & p_3^*(\tau_1, r_{23}) \triangleq \min_{\mathbf{W}_{23} \succeq \mathbf{0}} \text{tr}(\mathbf{W}_{23}) \\ & \text{s.t. } \mathbf{h}_2^H \mathbf{W}_{23} \mathbf{h}_2 \geq \gamma_{23}(\tau_1, r_{23}), \quad (23) \\ & \mathbf{h}_1^H \mathbf{W}_{23} \mathbf{h}_1 \geq e_1, \quad (24) \\ & \text{tr}(\mathbf{W}_{23}) \leq P_P(1 - \tau_1). \quad (25) \end{aligned}$$

$$(P1) : p_A^* = \min_{\{0 \leq \tau_i \leq 1, \{r_{ij} \geq 0\}\}} p_1^*(\tau_2, r_{11}) + p_2^*(\{\tau_i\}, \{r_{i2}\}) + p_3^*(\tau_1, r_{23})$$

$$s.t. r_{11} + r_{12} \geq \alpha r_{sum}, r_{22} + r_{23} \geq (1 - \alpha) r_{sum}, \tau_1 + \tau_2 \geq 1, \quad (13)$$

$$\gamma_{11}(\tau_2, r_{11}) \leq \gamma_{11}^{\max}(\tau_2), \tau_2 \leq 1 - \frac{e_2}{P_P \|\mathbf{h}_2\|^2}, \quad (14)$$

$$\gamma_{12}(\{\tau_i\}, r_{12}) \leq \gamma_{12}^{\max}(\{\tau_i\}, \{r_{i2}\}), \gamma_{22}(\{\tau_i\}, r_{22}) \leq P_P(\tau_1 + \tau_2 - 1) \|\mathbf{h}_2\|^2, \quad (15)$$

$$\gamma_{23}(\tau_1, r_{23}) \leq \gamma_{23}^{\max}(\tau_1), \tau_1 \leq 1 - \frac{e_1}{P_P \|\mathbf{h}_1\|^2}, \quad (16)$$

Also,  $\{\gamma_{ij}^{\max}(\cdot)\}$  in (14)-(16) are respectively given by

$$(P1.4) : \gamma_{11}^{\max}(\tau_2) \triangleq \max_{\mathbf{W}_{11} \succeq \mathbf{0}} \mathbf{h}_1^H \mathbf{W}_{11} \mathbf{h}_1, \quad s.t. (18), (19),$$

$$(P1.5) : \gamma_{12}^{\max}(\{\tau_i\}, \{r_{i2}\})$$

$$\triangleq \max_{\{\mathbf{W}_{i2} \succeq \mathbf{0}\}} \mathbf{h}_1^H \mathbf{W}_{12} \mathbf{h}_1 - \frac{\gamma_{12}(\{\tau_i\}, r_{12})}{\tau_1 + \tau_2 - 1} \mathbf{h}_1^H \mathbf{W}_{22} \mathbf{h}_1, \quad s.t. (21), (22),$$

$$(P1.6) : \gamma_{23}^{\max}(\tau_1) \triangleq \max_{\mathbf{W}_{23} \succeq \mathbf{0}} \mathbf{h}_2^H \mathbf{W}_{23} \mathbf{h}_2, \quad s.t. (24), (25).$$

*Proof:* See Appendix A ■

Theorem 1 shows that the original non-convex problem (7) can be optimally solved via (P1) and its subproblems (P1.1)-(P1.6). Note that (P1.1), (P1.2), and (P1.3) design the optimal transmit covariance matrices  $\{\mathbf{W}_{ij}^*\}$  for phase  $j = 1, 2$ , and 3 with fixed  $\{r_{ij}\}$  and  $\{\tau_i\}$ , and the corresponding optimal values  $\{p_j^*(\cdot)\}$  stand for the transmit energy consumed in phase  $j$ . With the optimal  $\{\mathbf{W}_{ij}^*\}$  at hand, (P1) finds the minimum average transmit power by optimizing the auxiliary variables  $\{r_{ij}\}$  and the TS ratios  $\{\tau_i\}$ . However, it is not easy to solve (P1) immediately due to the complicated objective and constraint functions  $\{p_j^*(\cdot)\}$  and  $\{\gamma_{ij}^{\max}(\cdot)\}$ . To tackle this issue, in Section III-A, we first address the subproblems for identifying  $\{p_j^*(\cdot)\}$  and  $\{\gamma_{ij}^{\max}(\cdot)\}$ . Then, the optimal  $\{\tau_i^*\}$  and  $\{r_{ij}^*\}$  for (P1) will be presented in Section III-B.

### A. Optimal Solution for Subproblems

In this subsection, we present the optimal solutions for (P1.1)-(P1.6). First, it can be shown that (P1.1)-(P1.3) are convex semi-definite programming (SDP), and their optimal solutions  $\{\mathbf{W}_{ij}^*\}$  are given by rank-one matrices [19]. Therefore, the functions  $\{p_j^*(\cdot)\}$  can be readily obtained by existing convex softwares, e.g., CVX.

Next, the optimal solutions of (P1.4) and (P1.6) can be determined in a closed-form expression [1], and the corresponding optimal values  $\gamma_{11}^{\max}(\tau_2)$  and  $\gamma_{23}^{\max}(\tau_1)$  are respectively derived as  $\gamma_{11}^{\max}(\tau_2) = g(\mathbf{h}_1, \mathbf{h}_2, P_P(1 - \tau_2), e_2)$  and  $\gamma_{23}^{\max}(\tau_1) = g(\mathbf{h}_2, \mathbf{h}_1, P_P(1 - \tau_1), e_1)$ , where

$$g(\mathbf{u}, \mathbf{v}, w, z) = \begin{cases} w \|\mathbf{u}\|^2, & \text{for } z \leq \frac{\mathbf{v}^H \mathbf{u}}{\|\mathbf{u}\|^2} w \\ \left( \frac{z}{\sqrt{\|\mathbf{v}\|^2}} \frac{\mathbf{v}^H \mathbf{u}}{\|\mathbf{u}\|^2} + \sqrt{w - \frac{z}{\|\mathbf{v}\|^2}} \|\mathbf{u}\| \right)^2, & \text{elsewhere} \end{cases} \quad (26)$$

with  $\mathbf{\Pi}_x^\perp \triangleq \mathbf{I}_m - \frac{\mathbf{x}\mathbf{x}^H}{\|\mathbf{x}\|^2}$  for a vector  $\mathbf{x} \in \mathbb{C}^{m \times 1}$  and  $\mathbf{I}_m$  being an identity matrix of size  $m$ -by- $m$ . In addition, we can calculate  $\gamma_{12}^{\max}(\{\tau_i\}, \{r_{i2}\})$  by solving the convex SDP in (P1.5).

### B. Proof for Convexity of (P1)

So far, the functions  $\{p_j^*(\cdot)\}$  and  $\{\gamma_{ij}^{\max}(\cdot)\}$  are identified by solving (P1.1)-(P1.6). In this subsection, we propose an approach for finding the optimal  $\{\tau_i^*\}$  and  $\{r_{ij}^*\}$  of the average

transmit power minimization problem (P1). We first provide the following lemmas which reveal the convexity of (P1).

*Lemma 1:* The functions  $p_1^*(\tau_2, r_{11})$ ,  $p_2^*(\{\tau_i\}, \{r_{i2}\})$ , and  $p_3^*(\tau_1, r_{23})$  are jointly convex.

*Proof:* See Appendix B. ■

*Lemma 2:* The functions  $\gamma_{11}^{\max}(\tau_2)$ ,  $\gamma_{12}^{\max}(\{\tau_i\}, \{r_{i2}\})$ , and  $\gamma_{23}^{\max}(\tau_1)$  are jointly concave.

*Proof:* The proof is similar to that of Lemma 1 and thus omitted for brevity. ■

It can be easily checked that the functions  $\gamma_{11}(\tau_2, r_{11})$ ,  $\gamma_{12}(\{\tau_i\}, r_{12})$ , and  $\gamma_{23}(\tau_1, r_{23})$  in constraints (14)-(16) are convex since the perspective operation preserves the convexity [20]. Combining this and Lemmas 1 and 2, we conclude that problem (P1) is jointly convex, whose globally optimal solution  $\{\tau_i^*\}$  and  $\{r_{ij}^*\}$  can be computed by the subgradient methods, e.g., the ellipsoid method [20]. To this end, we require the subgradients of the objective and the constraint functions  $\{p_j^*(\cdot)\}$  and  $\{\gamma_{ij}^{\max}(\cdot)\}$ . By utilizing the closed-form expressions of  $\gamma_{11}^{\max}(\tau_2)$  and  $\gamma_{23}^{\max}(\tau_1)$  in Section III-A, we can easily determine their subgradients with respect to each variable  $\{\tau_i\}$  and  $\{r_{ij}\}$ .

To calculate the subgradients of the remaining functions  $\{p_j^*(\cdot)\}$  and  $\gamma_{12}^{\max}(\{\tau_i\}, \{r_{i2}\})$ , whose exact derivations are not given in general, we need to investigate the dual functions of (P1.1)-(P1.3) and (P1.5), respectively. First, let us focus on the function  $p_2^*(\{\tau_i\}, \{r_{i2}\})$ . Notice that the subgradient of the pointwise maximum of convex functions equals that of the functions which achieves the maximum. Thus, it is not difficult to show from (36) in Appendix B that the subgradients  $\partial_x p_2^*(\{\tau_i\}, \{r_{i2}\})$  of  $p_2^*(\{\tau_i\}, \{r_{i2}\})$  with respect to each variable  $x \in \{\tau_i\} \cup \{r_{i2}\}$  are expressed by

$$\begin{aligned} & \partial_x p_2^*(\{\tau_i\}, \{r_{i2}\}) \\ &= \begin{cases} \mu_2^* v(r_{12}, \tau_1 + \tau_2 - 1) + \lambda_2^* v(r_{22}, \tau_1 + \tau_2 - 1), & \text{for } x = \tau_1 \text{ or } \tau_2, \\ \mu_2^* \exp\left(\frac{r_{12}}{\tau_1 + \tau_2 - 1}\right), & \text{for } x = r_{12}, \\ \lambda_2^* \exp\left(\frac{r_{22}}{\tau_1 + \tau_2 - 1}\right), & \text{for } x = r_{22}, \end{cases} \end{aligned}$$

where  $\mu_2^*$  and  $\lambda_2^*$  equal the optimal dual variable of (P1.2) associated with the constraints in (20) and (21), and  $v(x, t) \triangleq (1 - \frac{x}{t}) \exp(\frac{x}{t}) - 1$ . In a similar way, we can obtain the subgradients of  $p_1^*(\tau_2, r_{11})$  and  $p_3^*(\tau_1, r_{23})$ .

Also, thanks to the convexity and the Slater's condition, the primal optimal  $\gamma_{12}^{\max}(\{\tau_i\}, \{r_{i2}\})$  of (P1.5) is identical to its dual optimal value. By employing a similar process given in Appendix B, the primal optimal value  $\gamma_{12}^{\max}(\{\tau_i\}, \{r_{i2}\})$  for (P1.5) can be represented by its dual optimal as

$$\gamma_{12}^{\max}(\{\tau_i\}, \{r_{i2}\}) = \min_{\theta \geq 0, \phi \geq 0} \phi P_P(\tau_1 + \tau_2 - 1) - \theta \gamma_{22}(\{\tau_i\}, r_{22}) \quad (27)$$

$$s.t. \mathbf{h}_1 \mathbf{h}_1^H - \theta \frac{\gamma_{22}(\{\tau_i\}, r_{22})}{\tau_1 + \tau_2 - 1} \mathbf{h}_2 \mathbf{h}_2^H - \phi \mathbf{I}_M \preceq \mathbf{0},$$

$$\theta \mathbf{h}_2 \mathbf{h}_2^H - \frac{\gamma_{12}(\{\tau_i\}, r_{12})}{\tau_1 + \tau_2 - 1} \mathbf{h}_1 \mathbf{h}_1^H - \phi \mathbf{I}_M \preceq \mathbf{0},$$

TABLE I  
OPTIMAL ALGORITHM FOR (P) FOR CASE 1

Initialize $r_{min}$ and $r_{max}$ for $r_{sum}^* \in [r_{min}, r_{max}]$ .
Repeat
Update $r_{sum} \leftarrow \frac{r_{min} + r_{max}}{2}$ .
Repeat
Compute $\{p_i^*(\cdot)\}$ and $\{\gamma_{ij}^{\max}(\cdot)\}$ .
Update $\{\tau_i\}$ and $\{r_{ij}\}$ using the ellipsoid method.
Until $\{\tau_i\}$ and $\{r_{ij}\}$ converge
If $p_A^* \leq P_A$
Set $r_{min} \leftarrow r_{sum}$ .
Else
Set $r_{max} \leftarrow r_{sum}$ .
Until $r_{sum}$ converges

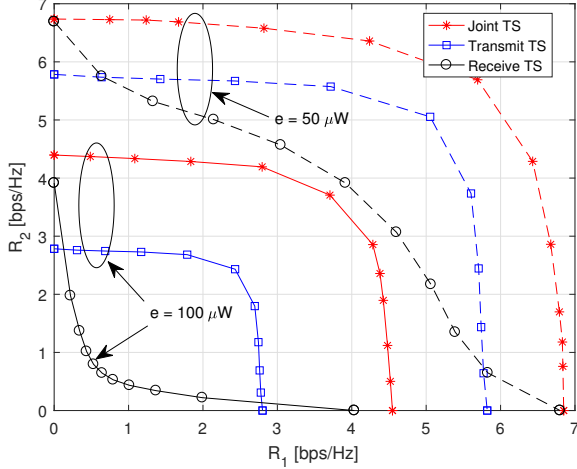


Fig. 3. Achievable rate regions of TS-based SWIPT schemes with  $M = 4$

where  $\phi$  and  $\theta$  are the dual variables corresponding to (21) and (22), respectively.

Since  $\gamma_{12}^{\max}(\{\tau_i\}, \{r_{i2}\})$  in (27) is the pointwise minimum of concave functions, its subgradient can be calculated as

$$\partial_x \gamma_{12}^{\max}(\{\tau_i\}, \{r_{i2}\}) = \begin{cases} \phi^* P_P - \theta^* v(r_{22}, \tau_1 + \tau_2 - 1), & \text{for } x = \tau_1 \text{ or } \tau_2, \\ 0, & \text{for } x = r_{12}, \\ -\theta^* \exp\left(\frac{r_{12}}{\tau_1 + \tau_2 - 1}\right), & \text{for } x = r_{22}, \end{cases}$$

where  $\phi^*$  and  $\theta^*$  indicate the optimal dual variables. The overall procedure for (P) for case 1 is summarized in Table I.

The optimal solutions for the remaining cases can also be computed by modifying the proposed algorithm in Table I. Due to the space limitation, the detailed approaches for solving (P) for other cases are omitted here and referred to [17].

#### IV. NUMERICAL EXAMPLES

In this section, we illustrate numerical results for various TS-based SWIPT systems and demonstrate the efficacy of the proposed joint TS protocol. For the simulations, we assume a carrier frequency of 900 MHz and 1 m distance from the transmitter to both the receivers, which results in 40 dB average signal attenuation [1]. The EH efficiency  $\zeta$  and the EH constraints  $\{e_i\}$  are fixed to  $\zeta = 0.5$  and  $e_1 = e_2 = e$ , respectively. Also, we employ  $P_A = P_P = 1$  W and the noise power of  $1 \mu\text{W}$ , respectively [4].

In Fig. 3, we compare the performance of the proposed joint TS protocol with conventional methods for  $M = 4$  with

different EH constraints  $e$ . Here, the channel vectors  $\mathbf{h}_i$  for  $i = 1$  and 2 are set to  $\mathbf{h}_i = \sqrt{10^{-4}} \tilde{\mathbf{h}}_i$ , where  $\tilde{\mathbf{h}}_i$  for  $i = 1, 2$  are defined in (28) and (29) on the top of the next page with  $\mathbf{j} \triangleq \sqrt{-1}$ . Here, the curves for the transmit TS scheme in [13] can be generated from the proposed algorithm for cases 3 and 4 with simple modifications, while for the receive TS, we utilize the method in [14]. From the figures, we can check that the achievable rate region of the proposed joint TS contains that of the conventional TS schemes regardless of  $e$ .

#### V. CONCLUSION

This paper has presented a new joint TS protocol for a two-user SWIPT MISO BC which includes the conventional transmit and receive TS schemes as special cases. We have investigated the achievable rate region of the joint TS system under the EH constraint at each receiver. The globally optimal algorithm has been provided which computes the optimal transmit covariance matrices and the optimal TS ratios. Numerical examples have demonstrated that the proposed joint TS outperforms the conventional TS schemes.

#### APPENDIX A PROOF OF THEOREM 1

Let us first show that the feasible region of  $\{r_{ij}\}$  and  $\{\tau_i\}$  can be represented by the constraints in (14)-(16) for any given finite peak power budget  $P_P < \infty$ . By applying (8)-(12), we can equivalently formulate (7) as

$$\begin{aligned} & \min_{\{\tau_i \geq 0\}, \{r_{ij} \geq 0\}, \{\mathbf{W}_{ij} \geq 0\}} \sum_{i=1}^2 \sum_{j=1}^3 \text{tr}(\mathbf{W}_{ij}), \\ & \text{s.t. (13), (17) - (25)}. \end{aligned} \quad (30)$$

One can check that with fixed  $\{r_{ij}\}$  and  $\{\tau_i\}$ , the problem in (30) can be decoupled into three subproblems in (P1.1)-(P1.3).

We first consider the feasibility of (P1.1). It is emphasized that  $\gamma_{11}^{\max}(\tau_2)$  in (P1.4) indicates the maximum value of  $\mathbf{h}_1^H \mathbf{W}_{11} \mathbf{h}_1$  under the EH and the peak power constraints (18) and (19). For this reason, it can be shown from (17) that feasible  $r_{11}$  and  $\tau_2$  must satisfy  $\gamma_{11}(\tau_2, r_{11}) \leq \gamma_{11}^{\max}(\tau_2)$ . Also, from (18), a feasible condition for  $\tau_2$  with a given  $P_P$  becomes

$$e_2 \leq \max_{\text{tr}(\mathbf{W}_{11}) \leq P_P(1-\tau_2)} \mathbf{h}_2^H \mathbf{W}_{11} \mathbf{h}_2 = P_P(1-\tau_2) \|\mathbf{h}_2\|^2.$$

Combining these results, we attain constraint (14). In a similar way, we can verify that (P1.2) and (P1.3) are feasible only when the constraints in (15) and (16) are satisfied, respectively.

Now, we prove the equivalence between (7) (or, equivalently (30)) and (P1). First, the optimal value of (P1) must be greater than that of (30) due to the additional constraints (14)-(16). Next, we will show that the optimal value of (P1) is smaller than that of (7). Let us denote  $\{\hat{\tau}_i\}$  and  $\{\hat{\mathbf{Q}}_{ij}\}$  as the optimal solution for (7). Also, we define  $\{\tilde{r}_{ij}\}$  as

$$\tilde{r}_{11} = (1 - \hat{\tau}_2) \log(1 + \mathbf{h}_1^H \hat{\mathbf{Q}}_{11} \mathbf{h}_1), \quad (31)$$

$$\tilde{r}_{i2} = (\hat{\tau}_1 + \hat{\tau}_2 - 1) \log\left(1 + \frac{\mathbf{h}_i^H \hat{\mathbf{Q}}_{i2} \mathbf{h}_i}{1 + \mathbf{h}_i^H \hat{\mathbf{Q}}_{i2} \mathbf{h}_i}\right), \text{ for } i = 1, 2, \quad (32)$$

$$\tilde{r}_{23} = (1 - \hat{\tau}_1) \log(1 + \mathbf{h}_2^H \hat{\mathbf{Q}}_{23} \mathbf{h}_2). \quad (33)$$

It is obvious that due to the constraints in (14)-(16),  $\{\tilde{r}_{ij}\}$  and  $\{\hat{\tau}_i\}$  which satisfy (31)-(33) must be feasible solutions

$$\tilde{\mathbf{h}}_1 = [-0.766 + 0.163j, -0.453 + 0.271j, 0.010 + 1.262j, -2.149 + 0.021j]^T, \quad (28)$$

$$\tilde{\mathbf{h}}_2 = [0.915 - 0.579j, 0.687 + 1.268j, -0.769 - 0.417j, -0.058 - 0.373j]^T, \quad (29)$$

for (P1). Then, the optimal value of (7) can be written by  $\Upsilon \triangleq p_1^*(\hat{\tau}_2, \hat{r}_{11}) + p_2^*(\{\hat{\tau}_i\}, \{\hat{r}_{i2}\}) + p_3^*(\hat{\tau}_1, \hat{r}_{23})$ , and it follows

$$\Upsilon \geq \min_{\{\tau_i \geq 0\}, \{r_{ij} \geq 0\}} p_1^*(\tau_2, r_{11}) + p_2^*(\{\tau_i\}, \{r_{i2}\}) + p_3^*(\tau_1, r_{23}).$$

This implies that the minimum of (P1) is smaller than that of (7). As a result, the optimal value of two problems (7) and (P1) are the same. This completes the proof.

## APPENDIX B PROOF OF LEMMA 2

We focus on showing the convexity of  $p_2^*(\{\tau_i\}, \{r_{i2}\})$  in this proof, and the convexity of other functions  $p_1^*(\tau_2, r_{11})$  and  $p_3^*(\tau_1, r_{23})$  can be directly verified in a similar way. Thanks to the constraint in (15), (P1.2) is always feasible for any finite  $P_P$ , i.e., with fixed  $\{\tau_i\}$  and  $\{r_{i2}\}$  satisfying (15), we have  $\text{tr}(\mathbf{W}_{12}^* + \mathbf{W}_{22}^*) \leq P_P(\tau_1 + \tau_2 - 1)$ . Thus, without loss of the optimality, the peak power constraint (22) in (P1.2) can be ignored. This relaxed problem is a convex SDP and satisfies the Slater's condition, which results in the strong duality [20]. Thus, the globally optimal solution for (P1.2) can be determined by the Lagrange duality method.

The Lagrangian is expressed as

$$\begin{aligned} \mathcal{L}_2(\{\mathbf{W}_{i2}\}, \mu_2, \lambda_2) &= \sum_{i=1}^2 \text{tr}(\mathbf{A}_i(\mu_2, \lambda_2) \mathbf{W}_{i2}) \\ &\quad + \mu_2 \gamma_{12}(\{\tau_i\}, r_{12}) + \lambda_2 \gamma_{22}(\{\tau_i\}, r_{22}), \end{aligned}$$

where  $\mu_2 \geq 0$  and  $\lambda_2 \geq 0$  stand for the dual variables associated with constraints (20) and (21), respectively, and  $\mathbf{A}_i(\mu_2, \lambda_2)$  for  $i = 1$  and  $2$  is defined as

$$\mathbf{A}_1(\mu_2, \lambda_2) \triangleq \mathbf{I}_M - \mu_2 \mathbf{h}_1 \mathbf{h}_1^H + \lambda_2 \frac{\gamma_{12}(\{\tau_i\}, r_{12})}{\tau_1 + \tau_2 - 1} \mathbf{h}_2 \mathbf{h}_2^H,$$

$$\mathbf{A}_2(\mu_2, \lambda_2) \triangleq \mathbf{I}_M - \lambda_2 \mathbf{h}_2 \mathbf{h}_2^H + \mu_2 \frac{\gamma_{22}(\{\tau_i\}, r_{22})}{\tau_1 + \tau_2 - 1} \mathbf{h}_1 \mathbf{h}_1^H.$$

The KKT optimality conditions are given by

$$\mathbf{A}_i^*(\mu_2^*, \lambda_2^*) \succeq \mathbf{0}, \text{ for } i = 1, 2, \quad (34)$$

$$\mathbf{A}_i^*(\mu_2^*, \lambda_2^*) \mathbf{W}_{i2}^* = \mathbf{0}, \text{ for } i = 1, 2, \quad (35)$$

$$\mu_2^* \left( \gamma_{12}(\{\tau_i\}, r_{12}) - \mathbf{h}_1^H \mathbf{W}_{12}^* \mathbf{h}_1 + \frac{\gamma_{12}(\{\tau_i\}, r_{12})}{\tau_1 + \tau_2 - 1} \mathbf{h}_1^H \mathbf{W}_{22}^* \mathbf{h}_1 \right) = 0,$$

$$\lambda_2^* \left( \gamma_{22}(\{\tau_i\}, r_{22}) - \mathbf{h}_2^H \mathbf{W}_{22}^* \mathbf{h}_2 + \frac{\gamma_{22}(\{\tau_i\}, r_{22})}{\tau_1 + \tau_2 - 1} \mathbf{h}_2^H \mathbf{W}_{12}^* \mathbf{h}_2 \right) = 0,$$

where (34) ensures that the dual function  $\mathcal{G}_2(\mu_2, \lambda_2) \triangleq \min_{\{\mathbf{W}_{i2} \succeq \mathbf{0}\}} \mathcal{L}(\{\mathbf{W}_{i2}\}, \mu_2, \lambda_2)$  has a bounded value.

Since the strong duality holds for (P1.2), its primal optimal value  $p_2^*(\{\tau_i\}, \{r_{i2}\})$  is identical to the dual optimal value, which is the maximum of the dual function  $\mathcal{G}_2(\mu_2, \lambda_2)$ . From (35), it follows

$$\begin{aligned} & p_2^*(\{\tau_i\}, \{r_{i2}\}) \\ &= \max_{\mu_2 \geq 0, \lambda_2 \geq 0} \mu_2 \gamma_{12}(\{\tau_i\}, r_{12}) + \lambda_2 \gamma_{22}(\{\tau_i\}, r_{22}), \quad (36) \\ & \text{s.t. (34)}. \end{aligned}$$

One can easily check that the objective function of problem (36) is jointly convex with respect to  $\{\tau_i\}$  and  $\{r_{i2}\}$ . Thus, the above dual problem can be interpreted as the pointwise maximization of a jointly convex function over  $\mu_2$  and  $\lambda_2$ , which preserves the convexity [20]. Consequently,  $p_2^*(\{\tau_i\}, \{r_{i2}\})$  is also a convex function. This completes the proof.

## REFERENCES

- [1] R. Zhang and C. K. Ho, "MIMO broadcasting for simultaneous wireless information and power transfer," *IEEE Trans. Wireless Commun.*, vol. 12, pp. 1989–2001, May 2013.
- [2] J. Xu, L. Liu, and R. Zhang, "Multiuser MISO beamforming for simultaneous wireless information and power transfer," *IEEE Trans. Signal Process.*, vol. 62, pp. 4798–4810, Sep. 2014.
- [3] C. Song, J. Park, B. Clerckx, I. Lee, and K.-J. Lee, "Generalized precoder designs based on weighted MMSE criterion for energy harvesting constrained multi-user MIMO channels," *IEEE Trans. Wireless Commun.*, vol. 15, pp. 7941–7954, Dec. 2016.
- [4] J. Park and B. Clerckx, "Joint wireless information and energy transfer in a  $K$ -user MIMO interference channel," *IEEE Trans. Wireless Commun.*, vol. 13, pp. 5781–5796, Oct. 2014.
- [5] H. Lee, S.-R. Lee, K.-J. Lee, H.-B. Kong, and I. Lee, "Optimal beamforming designs for wireless information and power transfer in MISO interference channels," *IEEE Trans. Wireless Commun.*, vol. 14, pp. 4810–4821, Sep. 2015.
- [6] Z. Zhu, Z. Chu, Z. Wang, and I. Lee, "Outage constrained robust beamforming for secure broadcasting systems with energy harvesting," *IEEE Trans. Wireless Commun.*, vol. 15, pp. 7610–7620, Nov. 2016.
- [7] H. Lee, C. Song, S.-H. Choi, and I. Lee, "Outage probability analysis and power splitter designs for SWIPT relaying systems with direct link," *IEEE Commun. Lett.*, vol. 21, pp. 648–651, Mar. 2017.
- [8] Q. Shi, L. Liu, W. Xu, and R. Zhang, "Joint transmit beamforming and receive power splitting for MISO SWIPT systems," *IEEE Trans. Wireless Commun.*, vol. 13, pp. 3269–3280, Jun. 2014.
- [9] Q. Shi, W. Xu, T.-H. Chang, Y. Wang, and E. Song, "Joint beamforming and power splitting for MISO interference channel with SWIPT: an SOCP relaxation and decentralized algorithm," *IEEE Trans. Signal Process.*, vol. 62, pp. 6194–6208, Dec. 2014.
- [10] Q. Shi, W. Xu, T.-H. Chang, Y. Wang, and E. Song, "Secrecy rate beamforming for multicell networks with information and energy harvesting," *IEEE Trans. Signal Process.*, vol. 65, pp. 677–689, Feb. 2017.
- [11] Z. Zhu, Z. Chu, Z. Wang, and I. Lee, "Joint optimization of AN-aided beamforming and power splitting designs for MISO secrecy channel with SWIPT," in *Proc. IEEE Int. Conf. Commun. (ICC)*, pp. 1–6, May 2016.
- [12] C. Shen, W.-C. Li, and T.-H. Chang, "Wireless information and energy transfer in multi-antenna interference channel," *IEEE Trans. Signal Process.*, vol. 62, pp. 6249–6264, Dec. 2014.
- [13] A. A. Nasir, H. D. Tuan, D. T. Ngo, T. Q. Duong, and H. V. Poor, "Beamforming design for wireless information and power transfer systems: receive power-splitting versus transmit time-switching," *IEEE Trans. Commun.*, vol. 65, pp. 876–889, Feb. 2017.
- [14] N. Janatian, I. Stupia, and L. Vandendorpe, "Joint MOO of transmit precoding and receiver design in a downlink time switching MISO SWIPT system," Available on-line at arXiv:1610.08290.
- [15] H. Lee, K.-J. Lee, H. Kim, B. Clerckx, and I. Lee, "Resource allocation techniques for wireless powered communication networks with energy storage constraint," *IEEE Trans. Wireless Commun.*, vol. 14, pp. 2619–2628, Apr. 2016.
- [16] H. Lee, K.-J. Lee, H.-B. Kong, and I. Lee, "Sum-rate maximization for multiuser MIMO wireless powered communication networks," *IEEE Trans. Veh. Technol.*, vol. 65, pp. 9420–9424, Nov. 2016.
- [17] H. Lee, K.-J. Lee, H. Kim, and I. Lee, "Joint transceiver optimization for MISO SWIPT systems with time switching," *submitted to IEEE Trans. Wireless Commun.*, Jul. 2017.
- [18] R. Zhang, Y.-C. Liang, C. C. Chai, and S. Cui, "Optimal beamforming for two-way multi-antenna relay channel with analogue network coding," *IEEE J. Sel. Areas Commun.*, vol. 27, pp. 699–712, Jun. 2009.
- [19] Y. Huang and D. P. Palomar, "Rank-constrained separable semidefinite programming with applications to optimal beamforming," *IEEE Trans. Signal Process.*, vol. 58, pp. 664–678, Feb. 2010.
- [20] S. Boyd and L. Vandenberghe, *Convex optimization*. Cambridge University Press, 2004.